Thermodynamic and Electron Diffraction Signatures of Charge and Spin Ordering in $La_{1-x}Ca_xMnO_3$

A. P. Ramirez, P. Schiffer,* S-W. Cheong, C. H. Chen, W. Bao,† T. T. M. Palstra, P. L. Gammel, D. J. Bishop, and B. Zegarski

Bell Laboratories, Lucent Technologies, 600 Mountain Avenue, Murray Hill, New Jersey 07974

(Received 1 June 1995)

The large-magnetoresistance compounds $La_{1-x}Ca_xMnO_3$ have been studied using specific heat, sound velocity (v), and electron diffraction. For $0.63 \leq x \leq 0.67$ charge ordering is observed at 260 K and accompanied by a dramatic ($>10\%$) increase in v. This simultaneous occurrence of electron and lattice ordering features implies extremely strong electron-phonon coupling, known to exist for the octahederally coordinated d^4 ion and originating in the Jahn-Teller effect. A dynamic manifestation of this Jahn-Teller coupling has been suggested by Millis *et al.* as the origin for colossal magnetoresistance. [S0031-9007(96)00020-8]

PACS numbers: 71.45.Lr, 71.38.+i, 75.30.Kz

The compounds $La_{1-x}Ae_xMnO_3$ where $Ae =$ Ca, Sr, Ba have recently been the subject of intense study due to their "colossal" magnetoresistance (CMR) near the Curie temperature [1]. Qualitatively, CMR arises from double exchange (DE) [2], a process where carrier hopping is greater between aligned spins than between antialigned spins due to the energy cost of flipping the carrier spin. Thus, a phase transition from a paramagnetic (PM) state to a ferromagnetic (FM) state is accompanied by a dramatic reduction in resistivity and subsequent CMR, given the usual magnetic field dependence of the Curie temperature T_c ($dT_c/dH > 0$). For $La_{1-x}Ca_xMnO_3$ this phenomenon occurs for $0.2 < x < 0.5$. For higher Ca concentrations, $0.5 < x < 1.0$, the ground state is antiferromagnetic (AF) [3] and nonmetallic [4] consistent with the DE idea.

Despite the success of DE theories in explaining the gross transport features in the manganites, on a quantitative level there are large gaps in our understanding. Millis, Shraiman, and Littlewood [5] have shown that DE alone cannot explain many features of the resistivity, perhaps the most obvious one being its magnitude, which is dramatically larger than theory predicts. Since high temperature conduction in the FM material involves displacement of a Jahn-Teller (JT) $3d^4$ ion by a $3d^3$ ion it is possible, as Millis, Shraiman, and Littlewood suggest, that electron-phonon coupling plays an important role in CMR. Indeed, it is known that the d^4 ion in an octahedral oxygen environment (dilute Cr^{2+} in MgO) does exhibit a large static JT effect [6] which is also thought to be the driving force for the large distortion of the perovskite structure in $LaMnO_3$ [7].

Just as DE theories have concentrated on the purely electronic degrees of freedom, most of our experimental understanding of $La_{1-x}Ca_xMnO_3$ [8] comes from measurements of charge and magnetic response through resistivity (ρ) and magnetization (M) [9]. In this Letter we present a systematic study of the specific heat (C) and sound velocity (v) as a function of temperature and calcium concentration (x) in order to gain insight into electron-lattice coupling from probes which do not couple directly to the electronic degrees of freedom. In the AF concentration region v undergoes a dramatic ($\approx 10\%$) hardening at a temperature coincident with previous observations of ρ and M anomalies (260 K). Electron diffraction shows superlattice reflections below 260 K, evidence that the primary order parameter is commensurate charge localization and not staggered magnetic moment. However, the change in v seen here at the CO transition temperature (T_{co}) is several orders of magnitude larger than seen at either typical AF transitions [10] or the CO transition in $La_{0.67}Sr_{0.33}NiO_4$ [11]—instead, its magnitude approaches changes common for ferroelectrics. This is evidence that extremely large electron-lattice coupling, coupled to a Jahn-Teller effect, exists in these materials, as suggested by theory.

The ceramic samples were synthesized using techniques described earlier [9]. Specific heat was measured using a standard semiadiabatic technique in either warming or cooling mode. The longitudinal sound velocity was measured in a homodyne configuration at either 5 or 10 MHz using $LiNbO_3$ transducers. Electron diffraction measurements were made with a JEOL 2000FX transmission electron microscope. Magnetization (dc) was measured with a SQUID magnetometer; resistivity was measured using a four probe as (17 Hz) in-line method; and thermopower was measured with a commercial (MMR) apparatus using a Constantan reference.

In Fig. 1(a) we show $C(T)$ for $x = 0.33$ and 0.63, concentrations where T_c and T_{co}, respectively, are maximized [7]. To compare the electronic contributions (ΔC) of the two samples, we must subtract a lattice contribution, and because the temperature range is of order the Debye temperature ($\theta_D \approx 500$ K [12]), the lattice part dominates. We find that in the region 50–320 K (shown in the inset) a set of three optical modes at energies $\varepsilon/k_B = 150$, 400, and 850 K fit the background well [13]. We see that for

 0031-9007/96/76(17)/3188(4)$10.00

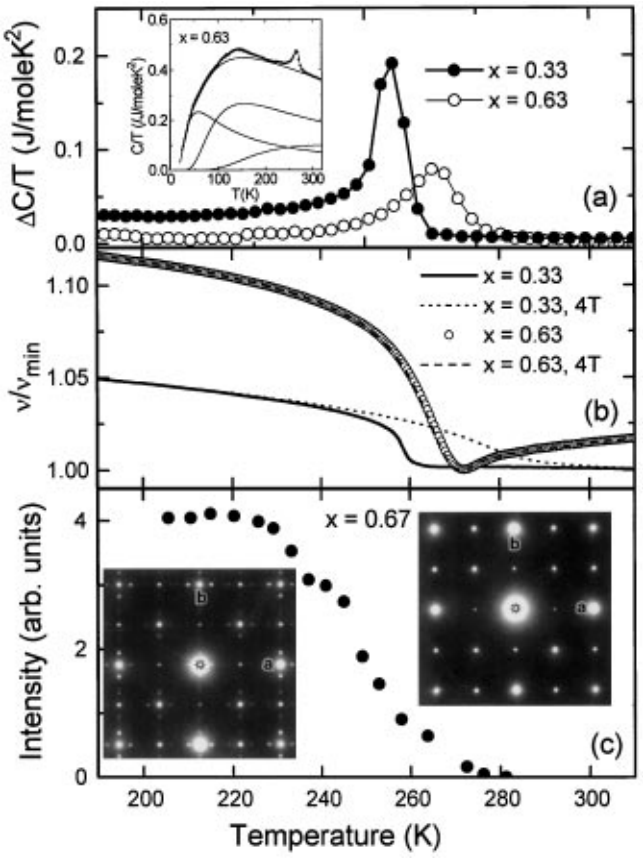

FIG. 1. (a, inset) Specific heat divided by temperature, C/T, for $x = 0.63$. The lines are three optical mode phonon contributions and their sum, approximating the lattice contribution. (a) C/T for $x = 0.33$ and 0.63 with lattice contribution subtracted from each. (b) Sound velocity, v, for $x = 0.33$ and 0.63. The dashed lines are v in a field of 4 T. (c, insets) Electron diffraction patterns for $x = 0.67$ material. Charge ordering is seen as superlattice spots as 200 K (left) in addition to the main spots seen at 300 K (right). The main Bragg spots labeled a and b can be indexed as (200) and (020), respectively. (c) Intensity of a representative Bragg spot at $\delta \approx 0.33$ versus temperature.

the $x = 0.63$ sample, besides the main anomaly at 265 K, there is an additional contribution at 145 K which is too sharp to be modeled by a single Einstein mode, and we discuss this feature below. This low temperature feature is not seen in the $x = 0.3$ sample which does, however, show a sharp peak associated with the FM transition at 260 K. The FM peak is narrower than previously seen for an $x = 0.2$ sample [12], possibly resulting from a small concentration gradient and a large T_c versus x slope.

In Fig. 1(b) we show the sound velocity versus temperature for both $x = 0.33$ and 0.63. At the FM transition for $x = 0.33$ we find an increase, Δv, of a few percent below T_c, an indication of strong coupling of sound to the internal energy, as seen in other ferromagnets [14]. The fractional increase in v observed for $x = 0.63$, which is not FM, is more than twice that of $x = 0.33$ below its phase transition. In addition, for $x = 0.63$, there is substantial softening as the transition is approached from higher temperatures, unlike the nearly temperature-independent behavior of $x = 0.33$ [15].

The large Δv ($\approx$10%) for $x = 0.63$ is surprising since the ground state is known to be AF and the inflection in $M(T)$ at 265 K is characteristic of an AF transition. Typical Δv's at such transitions are, however, of the order $<$0.1% [16]. Here, Δv is greater than usually observed even in charge-density-wave systems—indeed its magnitude is typical of ferroelectrics such as $BaTiO_3$ [16]. To better characterize the charge ordering, electron diffraction measurements were performed on several samples in the range $x = 0.63$–0.67. Figure 2(c) shows, for an $x = 0.67$ sample, data typical of this concentration range. The insets show diffraction patterns of the $(h\ k\ 0)$ zone of the reciprocal lattice taken at 200 and 300 K. At 300 K the diffraction pattern is consistent with the known $Pbnm$ orthohombic structure and lattice parameters $a \approx b \approx 5.5$ Å [3]. Below T_{co} [17], however, additional superlattice spots develop with an intensity shown in Fig. 1(c) and a modulation wave vector $\vec{q} = (2\pi/a)(\delta, 0, 0)$ with $\delta \approx 0.3$. The value of δ is found to vary from grain to grain between 0.33 and 0.30, although the commensurate value of 0.33 is frequently observed. The two orthogonal sets of superlattice spots are found to originate from different areas of the same grain suggesting a single $\vec{q}$, double-domain structure of the charge modulation.

Charge ordering of the type described here for $x \approx 0.63$ is of a different class then usual charge-density-wave (CDW) materials. The typical CDW transition is related to Fermi-surface nesting, and the development of a gap at the Fermi level leads to dramatic changes in the resistivity, but only small changes in the thermal and magnetic responses at T_{co}. In the present case, where high temperature conduction is via incoherent hopping, the resistivity change at T_{co} is in its temperature derivative while magnetic and thermal anomalies are large, reminiscent of transitions among localized moments. The best understood among this class of CO materials is the quasi-two-dimensional compound $La_{0.67}Sr_{0.33}NiO_4$ where a modulation wave vector of $\delta = 0.33$ (measured from the π,π point) is observed below its $T_{co} = 240$ K [18]. Recent thermodynamic measurements on $La_{0.67}Sr_{0.33}NiO_4$ exhibit shapes of Δv and ΔC similar to that seen for $La_{0.33}Ca_{0.67}MnO_3$ [11], suggesting a similar microscopic origin for the order-disorder transition. However, one striking difference between the two compounds is the magnitude of Δv—in the nickelate compound Δv is 2 orders of magnitude smaller than in the manganites. The most obvious source of this difference is the magnitude of the JT effect in both cases. While the JT splitting is significant for d^4 ions such as Mn^{3+} in an octahedral oxygen environment, EPR studies have shown there to be effectively no JT splitting for d^7 ions, such as Ni^{3+} [19]. Thus

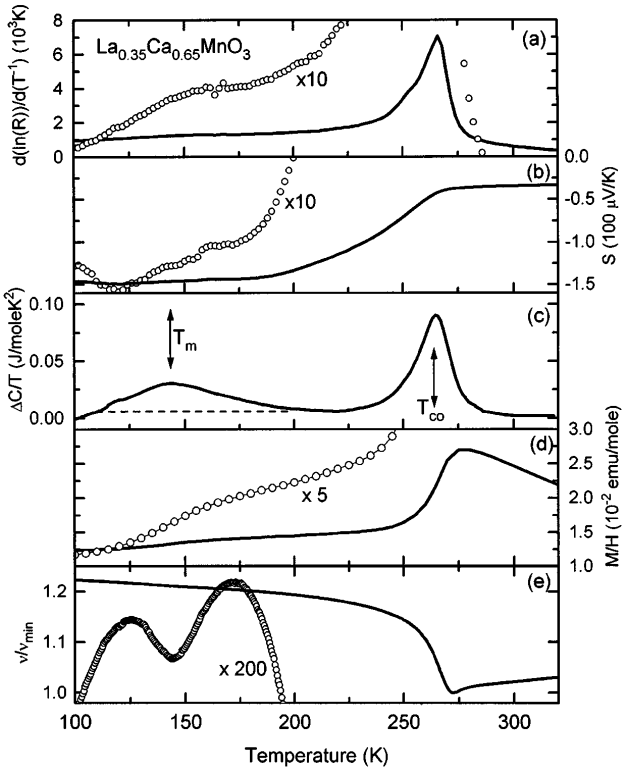

FIG. 2. Bulk transport and magnetic and thermal properties for $x = 0.65$ material as a function of temperature. (a) Logarithmic derivative, $d(\ln\rho)/d(T^{-1})$, of the resistivity. (b) Thermopower. (c) Specific heat divided by temperature with lattice estimate subtracted. (d) Magnetization divided by field. (e) Sound velocity (the magnified data are presented with a linear least-squares fit in the region 100–200 K subtracted). The charge-ordering transition temperature is $T_{co} = 265$ K.

it seems natural to ascribe the huge lattice hardening in the CO manganites to large electron-phonon coupling via the JT effect.

To further characterize the charge-ordering transition and the lower temperature feature seen in $C(T)$, we performed a series of thermodynamic and transport measurements shown in Fig. 2 on an $x = 0.65$ sample. In all the measurements, ρ, M, C, v, and thermopower, S, the temperature dependence is dominated by a feature at the charge-ordering transition, $T_{co} = 265$ K. The resistivity [Fig. 2(a)], plotted as $d(\ln R)/d(T^{-1})$, shows, in addition to a large peak at T_{co}, a smaller feature near 140 and activated behavior at lower T. The $T = 140$ K feature is not seen, however, in $S(T)$ [Fig. 2(b)]. Rather $S(T)$ exhibits a factor of 4 increase on passing through T_{co} from a value $-35\ \mu$V/K to another nearly T-independent value of $-150\ \mu$V/K, consistent with localization of charge carriers. We note that the behavior of $S(T)$ around 100 K is inconsistent with either hopping ($\sim T^{1/2}$) or semiconducting ($\sim T^{-1}$) transport, suggesting a more complicated mechanism. The peak in $C(T)$ [Fig. 2(c)] at 265 K apparently arises from critical fluctuations of the order-disorder type associated with charge ordering. A lower bound on the entropy developed at the 140 K transition, estimated by the area bounded by the data and the dashed line, is 1.2 J/mole K, a sizable fraction of the residual spin entropy, assuming the polarons do not spin order at T_{co}. The magnetization [Fig. 2(d)] undergoes a sharp decrease at T_{co}, as previously reported [9]. Careful inspection of the data shows a second drop in $M(T)$ around 140 K consistent with a transition to an AF state. Finally, magnification of $v(T)$ [Fig. 2(e)] also shows a pronounced feature near 140 K, of the size and shape commonly found for AF transitions [10]. All of these data taken together strongly suggest that the lower transition occuring at $T_m \approx 140$ K is from a PM state to an AF state. Although we cannot immediately rule out the existence of short range AF order between T_m and T_{co}, the large entropy loss at T_m suggests this is the primary magnetic transition and not a simple reorientation of the AF wave vector.

To complete the thermodynamic characterization we performed a series of $C(T)$ measurements for several different samples in the temperature region 50–320 K. In Fig. 3 $C(T)$ is shown for the concentrations $x = 0.1, 0.33, 0.5, 0.63, 0.65, 0.75$, and 0.9, each with the approximate

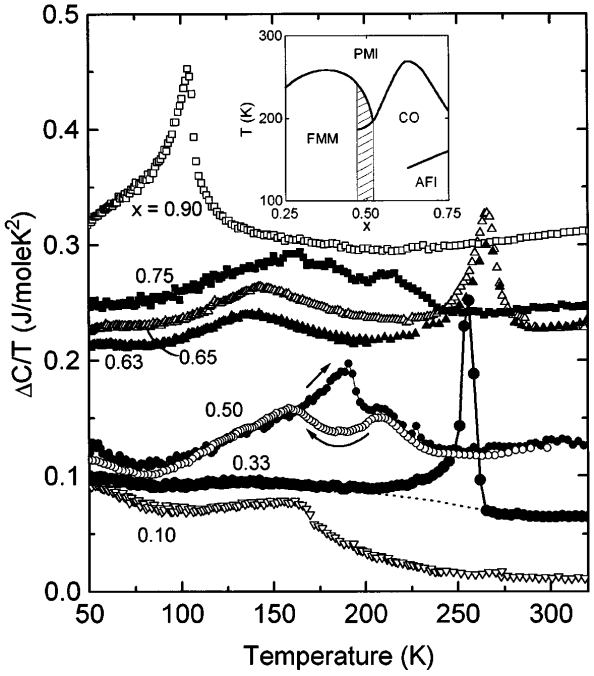

FIG. 3. Specific heat divided by temperature with the lattice estimate subtracted, for concentrations $x = 0.10$, 0.33, 0.50, 0.63, 0.65, 0.75, and 0.90. The data have been offset by 0, 0.06, 0.11, 0.12, 0.22, 0.26, and 0.33 mJ/mole K^2, respectively, for clarity. The data for $x = 0.50$ were taken as a function of both increasing and decreasing temperatures, as shown by the arrows. The inset shows a schematic of the new phase diagram for $La_{1-x}Ca_xMnO_3$, based on the present data and those of Ref. [7]. Here PMI, FMM, CO, and AFI denote paramagnetic insulating, FM metal, charge ordered, and AF insulating states, respectively. The hatched region indicates the uncertainty in the Ca-concentration value delineating the FM and AFM phases.

lattice contribution shown in the inset of Fig. 1(a) subtracted. At $x = 0.1$ and 0.9 we see signatures of FM and AF transitions, respectively, the former broadened perhaps as a result of proximity of T_c to the metal-insulator boundary. In the CMR regime, FM ordering is evident as a sharp, asymmetric peak with approximately $0.4R\ln 2$ entropy developed in the region bounded by the data and the dotted line. This value is consistent with the simultaneous loss of approximately $1/2R\ln 5$ (this being the estimated entropy due to the FM ordering of the Mn $S = 2$ ions—the factor $1/2$ accounts for spin wave depopulation below 200 K) and a gain of about 2.5 J/mole K^2 from delocalization of the doped electrons at T_c (we estimated this from the value of γ at low T integrated up to 250 K [20]). At $x = 0.50$ we find clear evidence for two phase transitions as seen in ρ and M studies [9]. The upper transition is FM, and T_c exhibits no difference depending on heating or cooling. The lower one has been ascribed to a simultaneous AF-charge ordering transition and exhibits clear hysteresis, with an undercooling or overcooling temperature difference similar to that seen in ρ and M. In the inset of Fig. 3 we show a schematic of a revised phase diagram for $La_{1-x}Ca_xMnO_3$ to illustrate the placement of the new phase boundaries corresponding to the AF transitions near 145 K.

Although most of the focus of CMR materials has been the FM phase at low doping, it is clear that the CO phase at high doping also has unusual properties, especially in its lattice response. The relevance of CO to the FM phase is that both phenomena arise from the same *local* physics, governed by the Hund and JT energies. Thus, the FM and CO states can be viewed as the limiting cooperative state of the same underlying system. It is clear that a comprehensive theory of CMR must also provide an accounting of CO and the present results should constrain any such theory.

We acknowledge useful conversations with G. Aeppli, P. Chandra, D. A. Huse, H. Y. Hwang, P. B. Littlewood, M. Marezio, A. J. Millis, P. Radaelli, and B. Shraiman.

*Permanent address: Physics Department, University of Notre Dame, Notre Dame, IN 46556.

†Present address: Physics Department, Brookhaven National Laboratory, Upton, NY 11973.

[1] S. Jin *et al.,* Science **264**, 413 (1994); R. von Helmolt *et al.,* Phys. Rev. Lett. **71**, 2331 (1993); K. Chahara *et al.*, Appl. Phys. Lett. **63**, 1990 (1993); R. M. Kusters *et al.*, Physica (Amsterdam) **155B**, 362 (1989).

[2] C. Zener, Phys. Rev. **82**, 403 (1951); P. G. de Gennes, Phys. Rev. **118**, 141 (1960).

[3] E. O. Wollan and W. C. Koehler, Phys. Rev. **100**, 545 (1955).

[4] G. H. Jonker and J. H. Van Santen, Physica (Utrecht) **16**, 337 (1950); **16**, 599 (1950).

[5] A. J. Millis, B. I. Shraiman, and P. B. Littlewood, Phys. Rev. Lett. **74**, 5144 (1995).

[6] J. R. Fletcher and K. W. H. Stephens, J. Phys. C **2**, 444 (1969).

[7] J. B. A. A. Elemans, J. Solid State Chem. **3**, 238 (1971).

[8] The compounds with $Ae =$ Ca are unique for the alkaline earths in that Ca can be continuously substituted over the whole concentration range.

[9] P. Schiffer, A. P. Ramirez, W. Bao, and S-W. Cheong, Phys. Rev. Lett. **75**, 3336 (1995), and references therein.

[10] C. W. Garland, in *Physical Acoustics*, edited by W. P. Mason and R. N. Thurston (Academic Press, New York, 1970), Vol. VII.

[11] A. P. Ramirez, P. L. Gammel, S-W. Cheong, D. J. Bishop, and P. Chandra, Phys. Rev. Lett. **76**, 447 (1996).

[12] J. Tanaka and T. Mitsuhashi, J. Phys. Soc. Jpn. **53**, 24 (1984).

[13] This phonon spectrum is consistent with that seen by inelastic neutron scattering in $(La,Pb)MnO_3$; G. Aeppli (private communication).

[14] G. A. Alers, J. R. Neighbours, and H. Sato, J. Phys. Chem. Solids **13**, 40 (1960).

[15] This behavior is not readily apparent from x-ray diffraction studies: P. G. Radaelli, D. E. Cox, M. Marezio, S-W. Cheong, P. E. Schiffer, and A. P. Ramirez, Phys. Rev. Lett. **75**, 4488 (1995); P. G. Radealli (private communication).

[16] D. Berlincourt and H. Jaffe, Phys. Rev. **111**, 143 (1958).

[17] The precise value of T_c cannot be determined from the intensity of TEM superlattice spots because of multiple scattering effects. In charge-density-wave systems, T_c is typically where the intensity first becomes observable.

[18] C. H. Chen, S-W. Cheong, and A. S. Cooper, Phys. Rev. Lett. **71**, 2461 (1993).

[19] A. Abragam and B. Bleaney, *Electron Paramagnetic Resonance of Transition Ions* (Dover Publications, New York, 1986).

[20] J. M. D. Coey, M. Viret, L. Ramo, and K. Ounadjela, Phys. Rev. Lett. **75**, 3910 (1995).